Computational and Structural Biotechnology Journal 18 (2020) 953–966

COMPUTATIONAL AND STRUCTURAL BIOTECHNOLOGY JOURNAL

journal homepage: www.elsevier.com/locate/csbj

Microvesicles from indoxyl sulfate-treated endothelial cells induce vascular calcification *in vitro*

Matilde Alique [a,*], Guillermo Bodega [b], Elena Corchete [c], Estefanya García-Menéndez [d], Patricia de Sequera [c], Rafael Luque [e], Daily Rodríguez-Padrón [e], María Marqués [d], José Portolés [d], Julia Carracedo [f,*,1], Rafael Ramírez [a,1]

[a] *Departamento de Biología de Sistemas, Universidad de Alcalá (IRYCIS), Alcalá de Henares, Madrid, Spain*
[b] *Departamento de Biomedicina y Biotecnología, Universidad de Alcalá, Alcalá de Henares, Madrid, Spain*
[c] *Sección de Nefrología, Hospital Universitario Infanta Leonor, Madrid, Spain*
[d] *Servicio Nefrología, Hospital Universitario Puerta de Hierro, Madrid, Spain*
[e] *Departamento de Química Orgánica, Universidad de Córdoba, Edificio Marie Curie (C-3), Carretera Nacional IV-A, Km 396, Córdoba, Spain*
[f] *Departamento de Genética, Fisiología y Microbiología, Facultad de Ciencias Biológicas, Universidad Complutense de Madrid/ Instituto de Investigación Sanitaria Hospital 12 de Octubre (imas12), Madrid, Spain*

ARTICLE INFO

Article history:
Received 24 January 2020
Received in revised form 2 April 2020
Accepted 5 April 2020
Available online 9 April 2020

Keywords:
Microvesicles
Uremic toxins
Endothelial cells
Vascular cells
Calcification

ABSTRACT

Vascular calcification (VC), an unpredictable pathophysiological process and critical event in patients with cardiovascular diseases (CVDs), is the leading cause of morbi-mortality and disability in chronic kidney disease (CKD) patients worldwide. Currently, no diagnostic method is available for identifying patients at risk of VC development; the pathology is detected when the process is irreversible. Extracellular vesicles (EVs) from endothelial cells might promote VC. Therefore, their evaluation and characterization could be useful for designing new diagnostic tools. The aim of the present study is to investigate whether microvesicles (MVs) from endothelial cells damaged by uremic toxin and indoxyl sulfate (IS) could induce calcification in human vascular smooth muscle cells (VMSCs). Besides, we have also analyzed the molecular mechanisms by which these endothelial MVs can promote VC development. Endothelial damage has been evaluated according to the percentage of senescence in endothelial cells, differential microRNAs in endothelial cells, and the amount of MVs released per cell. To identify the role of MVs in VC, VSMCs were treated with MVs from IS-treated endothelial cells. Calcium, inflammatory gene expression, and procalcification mediator levels in VSMCs were determined. IS-treated endothelial cells underwent senescence and exhibited modulated microRNA expression and an increase in the release of MVs. VSMCs exposed to these MVs modulated the expression of pro-inflammatory genes and some mediators involved in calcification progression. MVs produced by IS-treated endothelial cells promoted calcification in VSMCs.

1. Introduction

The leading cause of endothelial dysfunction, which dominates the landscape of chronic kidney disease (CKD) patients, is the accumulation of uremic toxins that damage the endothelium. It is well-known that endothelial cell dysfunction is implicated in the development of cardiovascular complications [1]. Vascular calcification (VC) is a frequent complication associated with the progressive deterioration of renal functions in CKD patients, and is a predictor of cardiovascular morbidity and mortality in these patients. No specific biomarker of VC has been discovered, and diagnosis exclusively involves radiological analyses [2]. Nevertheless, accumulating evidence supports the fact that the production of altered extracellular vesicles (EVs) by endothelial cells could at least partially explain how damage suffered by the endothelial cell extends to the rest of the cells in the vascular vessel [3] and could contribute to calcium accumulation in the vessel walls.

EVs are subcellular structures produced by most cells under physiological and stress conditions. EVs are subdivided into 3

* Corresponding authors at: Universidad de Alcalá (IRYCIS), Facultad de Medicina y Ciencias de las Salud. Departamento Biología de Sistemas, E-28871, Alcalá de Henares, Madrid, Spain (M. Alique).
E-mail address: matilde.alique@uah.es (M. Alique).
[1] These authors share senior authorship.

https://doi.org/10.1016/j.csbj.2020.04.006

types, including highlighted microvesicles (MVs), also known as microparticles [4]. MVs play an active physiological role in regulating the intercellular network involved in tissue reparation and homeostasis. However, under pathological conditions, altered cells might release a different number of MVs with an altered phenotype and/or atypical cargo, thereby promoting changes in other cells in adjacent tissues [5–7]. Consequently, MVs produced by endothelial cells have attracted particular interest, as they can be quantified in peripheral blood and be used as a biomarker for endothelial damage [8–10]. Their characterization might provide information about the mechanism by which endothelial cells could cause vascular injury and cardiovascular disease (CVD) [11,12].

MVs released by different cells initiate the cascade of events that culminate with the osteogenic transformation of vascular cells [13]. Endothelial cells, in particular, produce MVs that act as a signal for the calcification process in vascular cells [10]. Moreover, vascular smooth muscle cells (VSMCs) become susceptible to MVs and undergo a progressive change in their phenotype [14]. In addition, VSMCs reportedly exhibit an inflammatory response that could mediate the calcification process [15,16].

Though a healthy endothelium modulates homeostasis in the vasculature, under pathological conditions, it induces an inflammatory response-, which results in endothelial damage that might be subsequently related to endothelial senescence [17,18]. Some studies have demonstrated that endothelial injury caused by inflammatory cytokines [17] and uremic toxins [19,20] induces the development of cellular senescence; therefore, it could modulate the production of altered endothelial MVs [21]. Moreover, cells from the vascular wall rely on MVs to carry out interactions with the extracellular environment, and such cells that interact with altered MVs from endothelial damaged cells might promote VC [10]. However, no studies have investigated the effect of MVs derived from endothelial cells exposed to uremic toxins, as observed in CKD patients.

VC is an irreversible and common phenomenon associated with elderly [10] and CKD [22] patients that actively contributes to the development of inflammatory CVD [23]. The early identification of VC in CKD patients or even in the previous steps of this calcification process, together with the understanding of the physiopathological mechanism of VC, could be essential for preventing CVD progression. Unfortunately, VC is a silent disorder [2,20] resulting because of the activity of a complex network of signals that regulate the process of bone mineralization, mainly in VSMCs, due to these cells becoming susceptible to these signals [24]. To date, knowledge regarding the cellular and molecular mechanisms involved in VC development is scarce.

This study aims to determine if a uremic toxin such as indoxyl sulfate (IS) could mediate endothelial damage with the subsequent production of MVs capable of promoting calcification in VSMCs. In addition, we have characterized the potential key elements associated with endothelial MVs and the procalcificant signals induced by these MVs on VSMCs. This approach could be useful as a diagnostic tool in future studies, for identifying patients at risk of VC and for developing new therapies.

2. Material methods:

2.1. Cell cultures

Human umbilical vein endothelial cells (HUVECs, CC-2517, lot number 323,352 Lonza) were cultured in EGM medium (Lonza) supplemented with 10% heat-inactivated fetal bovine serum (FBS; Sigma). Cultures were maintained at 37 °C under 5% CO_2 conditions at 95% humidity in the EGM medium, which was comprised of endothelial basal media (EBM; Lonza CC-3121), supplemented with a growth bullet kit (Lonza, CC-4133) containing bovine brain extract, ascorbic acid, hydrocortisone, epidermal growth factor, gentamicin/amphotericin-B, and 10% heat-inactivated FBS. Experiments involving HUVECs were performed in cells passaged < 9 times (PD < 20). The rate of population doubling (PD), which occurred between passages was calculated using the formula PD = [ln {number of cells harvested} – ln {number of cells seeded}]/ln2].

Human aortic smooth muscle cells (HASMCs, CC-2571) were obtained from Lonza. Cells were maintained in the SmGM-2 medium (Lonza; CC-3181) supplemented with 20% FBS (Sigma) at 37 °C in a humidified atmosphere containing 5% CO_2. HASMCs from passage 5–7 were used in the experiments.

2.2. Experimental design in IS-treated HUVECs

HUVECs were seeded the day before (day 0) treatment was to be carried out in EGM medium (Lonza) supplemented with 10% heat-inactivated FBS (Sigma). The following day (day 1), endothelial cells were treated with IS (indoxyl sulfate; Sigma) dissolved in DMSO (Sigma) 250 μM for 3 days. On day 4, the media for the HUVECs were changed, and on the following day (day 5), media were collected (Fig. 1). Supernatants from each experiment were pooled, and MVs were isolated as described below. In addition, control and IS-treated HUVECs were stained, for testing the β-galactosidase (SA-β-gal) activity, as described further.

2.3. Isolation, quantification, and characterization of microvesicles

MVs from IS-treated endothelial cells were isolated. Briefly, cell culture supernatants were serially centrifuged (15 min at 3,000 rpm to remove cells and cellular debris, 30 min at 14,000 rpm to concentrate the MVs in Eppendorf centrifuges), as described by the International Society on Thrombosis and Haemostasis [25]. Pooled MVs from control and IS-treated HUVEC cultures were characterized following International Society for Extracellular Vesicles (ISEV) guidelines [26], using confocal microscopic analysis for size control, and flow cytometry for quantifying and analyzing membrane markers by mass spectrometry analysis [27]. Confocal microscopy analysis results showed that MVs ranged in size from 0.3 to 1.2 μm. Pooled MVs from control and IS-treated endothelial cells were mixed in equal amounts and after that they were characterized and quantified in terms of size, using the Beckman Coulter Cytomic FC 500 flow cytometer, with CXP software. The occurrence of MVs was understood to be gated events and their size was assessed from a side scatter (SSC) *vs*. forward scatter (FSC) dot-plot, which was produced in a standardization experiment using the SPHERO™ Flow Cytometry Nano Fluorescent Size Standard Kit (Spherotech). The latter has size-calibrated fluorescent beads ranging in size from 0.22 to 1.35 μm in diameter. Events in which the size was less than 0.22 μm were adequately excluded while distinguishing real events from those in the background; events in which the size was >1.35 μm were excluded, to prevent them from possibly being confused with apoptotic bodies [28]. Mass spectrometry analysis was performed as previously described [27], and showed the presence of different proteins that in the ISEV guidelines are suggested as markers for the four categories of proteins that are recommended should be checked: tetraspanin and lactadherin (category 1), annexins and syntenin (category 2), cytochrome *c* and HSP90B1 (category 3), and fibronectin, collagen α and MMP14 (category 4).

Moreover, MVs from the HUVEC culture medium were characterized with regard to their protein profiles, as shown below. Double-fluorescent labeling was performed to confirm the protein profile of the MVs obtained from HUVECs. Characterization was performed by incubating endothelial MVs with fluorescein

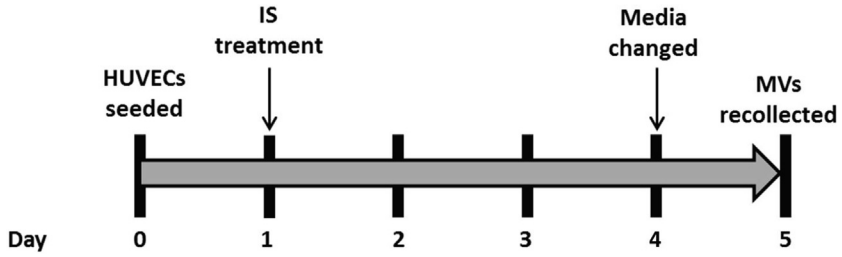

Fig. 1. Schematic diagram of the experimental design to obtain for endothelial cells (HUVECs) model.

isothiocyanate-conjugate (FITC) labeled monoclonal anti-CD31 (BD Pharmingen) and phycoerythrin-annexin A5 (BD Pharmingen), in annexin A5-biding buffer (10 mM HEPES, 7.4 pH, 140 mM NaCl, 2.5 mM $CaCl_2$). An equal volume of Flow-Count calibration beads (Beckman Coulter) was added to measure the number of events per microliter. Isotype negative controls were also prepared. A sample with fluorescein-conjugated annexin A5 and a $CaCl_2$-free solution was used as a control for annexin A5 labeling. To confirm the exclusion of apoptotic bodies during MVs isolation, the DNA content of the HUVEC-derived MVs was determined, by incubating them with acridine orange (Invitrogen), till a final concentration of 20 mM was achieved.

2.4. Analysis of senescence-associated β-galactosidase (SA-β-gal) activity

SA-β-gal staining was performed using the senescence-galactosidase staining kit (Abcam, Catalog #ab65351), according to the manufacturer's protocol. In brief, on day 5, control and IS-treated endothelial cells were washed with PBS and fixed in fixing solution for 12 min at room temperature. Next, they were washed in PBS to remove the fixing solution and incubated in freshly prepared SA-β-gal at 37 °C for 16 h without CO_2. At the end of the incubation period, SA-β-gal-positive cells (senescent cells) were identified as blue-stained cells under a standard light microscope. The number of blue colored positive cells was counted and normalized to the number of total cells in the same field. The percentage of SA-β-gal-positive cells was calculated in 8 randomly selected microscopic fields (magnification 100X).

2.5. Electron microscopy

For the microanalysis of ions, SEM-EDX (Scanning Electron Microscopy-Energy Dispersive Microanalysis System) analysis was performed, using the JEOL-SEM JSM-7800 LV scanning microscope. Prior to analysis, MVs samples were diluted in PBS, placed under coverslips, allowed to dry at room temperature, and further fixed in 2% glutaraldehyde for 24 h, at 4 °C. Subsequently, the MVs were dehydrated in ethanol and dried using the routine critical point drying procedure for SEM analysis. The prepared MVs were platinum coated (1.5 nm) in a Polaron E5400 metal evaporator (BioRad).

2.6. Treatment of HAMCs with MVs and determination of mineralization levels

HASMC mineralization levels were analyzed via qualitative staining, using alizarin red. HASMCs (10000 cells/well, 24-well plates) were cultured with 50,000 MVs/mL from the control and IS-treated HUVECs groups for 9, 20, and 30 days in 2% FBS-supplemented DMEM. Cells exposed to 2% FBS-supplemented DMEM containing 2.0 mM inorganic phosphorus (Pi; pro-calcifying condition) were used as a positive control. Culture medium was renewed every 2 days. The detection and quantification of mineral deposits was performed via alizarin red staining. Briefly, samples were fixed (50% ethanol 5 min, 95% ethanol 5 min), stained for 5 min with alizarin red S (40 mM, pH 4.2; Sigma), rinsed with 50% ethanol, and subsequently scanned. At the end of the incubation period, images of cells stained with alizarin red S were captured using a phase-contrast inverted light microscope (Optika; magnification 100X).

2.7. Assessment of calcium deposits

After an incubation period of 30 days, mineralization levels were determined. Cells were decalcified with 0.6 N HCl overnight at 4 °C. The calcium content of supernatants was determined by spectrophotometry, using a kit containing phenolsulphonephthalein dye (no. DICA-500, QuantiChrom calcium assay kit; BioAssay Systems). Then, cells were washed three times with PBS (Sigma) and solubilized in 0.1 M NaOH/1% SDS. The protein content was measured using the BCA protein assay kit (Pierce), and the calcium content was normalized to the total protein content. The calcium content in the cells was expressed in terms of μg/mg protein.

2.8. Real-time PCR

Total RNA was extracted from control and IS-treated HUVECs, as well as MVs-treated HASMCs using the mirVana PARIS RNA and Native Protein Purification Kit (Ambion), according to the manufacturer's instructions. cDNA was synthesized using the High Capacity cDNA Archive Kit (Applied Biosystems, Foster City, California, USA), using 2 μg of total RNA primed with random hexamer primers, as per the manufacturer's instructions. Real-time polymerase chain reactions (PCR) were performed using the ABI Prism 7500 sequence detection PCR system (TaqMan® Universal Master Mix II, No AmpErase® UNG; Applied Biosystems), as per the manufacturer's protocol. The assay IDs used were as follows: Runx2, Hs001047973_m1, BMP2, Hs00154192_m1, TWEAK (Hs00387540_g1), CCL2 (Hs002344140_m1), CCL5 (Hs00982282_m1), TNF-α (Hs00174128_m1) and, IL-6 (Hs00174131_m1) and, HPRT1, Hs02800695_m1 (as normalized assay). The mRNA copy numbers were calculated for each sample with instrument software, using a comparative threshold (Ct) value. The relative fold-change was determined using $2 - \Delta\Delta Ct$ methods, using control MVs-treated HASMCs as the baseline; their levels were normalized to HPRT1 expression levels.

2.9. Real-time PCR of mature microRNAs

Total RNA was extracted from control and IS-treated HUVECs. Total RNA was isolated using the mirVana PARIS RNA and Native Protein Purification Kit (Ambion), according to the manufacturer's instructions. The miRNA targets were reverse transcribed using a pool of RT primers obtained from TaqMan Small RNA Assays (Applied Biosystems) and total RNA, using the TaqMan MicroRNA

Reverse Transcription Kit (Applied Biosystems). Reaction tubes were kept on ice for at least 5 min, followed by incubation in a thermal cycler at 16 °C for 30 min, 42 °C for 30 min, 85 °C for 5 min, and were kept at 4 °C. A micro-NTC (no-template control) that contained no sample RNA was included in these reverse-transcription reactions. Subsequently, quantitative real-time PCR was performed in a PCR reaction mixture using the 20 × TaqMan miR Assay, which included PCR primers and probes (5′-FAM), and 2 × TaqMan Universal Master mix with no UNG (Applied Biosystems) and RT products. The reaction mixture was first incubated at 95 °C for 10 min, followed by 40 cycles at 95 °C for 15 s and 60 °C for 1 min. The following assay IDs were used: hsa-miR-126-3p (assay ID 002228), hsa-miR-126-5p (assay ID 000451), hsa-miR-155 (assay ID002623), hsa-miR-21-3p (assay ID 000397), hsa-miR-21-5p (assay ID 002438), hsa-miR-210 (assay ID 000512), hsa-miR-125b (assay ID 000449), hsa-miR-150 (assay ID 000473), hsa-miR-1915 (assay ID 121111_mat), hsa-miR-601 (assay ID 001558), hsa-miR-575 (assay ID 001617), and U6 snRNA (assay ID 001973); all these materials were purchased from Applied Biosystems. The relative amounts of each miRNA were calculated using the comparative threshold (Ct) method, by determining the ΔCt, Ct(miRNA) − Ct(U6 snRNA) values in endothelial cells. The miRNA copy numbers were calculated for each sample with instrument software, using Ct values. The relative miRNA expression level was calculated using the $2 - \Delta\Delta Ct$ method, using control HUVECs as the baseline, whose levels were normalized to U6 snRNA (internal control miRNAs) expression levels.

2.10. Western blot analyses

Extracts from control, IS-treated endothelial cells, as well as controls and MVs-treated HASMCs were lysed using the CytoBuster Protein Extraction Reagent lysis buffer (Millipore), containing a protease and phosphatase inhibitor cocktail (Roche). The total protein content of the lysates was quantified using a BCA Protein Assay Kit (Pierce), using BSA as a standard. Briefly, equal amounts of proteins (20–50 μg protein/lane) were diluted with the reducing sample buffer and separated via SDS/PAGE (10% gel), under reducing conditions. Samples were then transferred onto nitrocellulose membranes (BioRad), blocked in TBS containing 0.1% Tween 20 and 5% dry non-fat milk for 1 h at room temperature. They were probed using the following primary antibodies in the same buffer, at different dilutions: Cyclin D1 (Thermo Scientific, Cat. No. RM-9104-SO, dilution 1/1000, 36 kDa), Lamin B1 (Abcam, ab133741, dilution 1/1000, 66 kDa), SM22α (Santa Cruz Biotechnology, sc-53932, dilution 1/500, 22 kDa), and GAPDH (Millipore, Cat No. MAB374, dilution 1/2000, 38 kDa); α-tubulin from Sigma (T5158; loading control) was used as a loading control. After washing, the membranes were incubated with Novex horseradish peroxidase-conjugated secondary antibodies (1:5000). Bands were visualized with the Luminata Crescendo Western HRP substrate (Millipore). The quality of proteins and efficacy of protein transfer was evaluated by Red Ponceau (Sigma) staining. Bands were quantified using Image J software (NIH) and protein levels were normalized to anti-GAPDH or anti- α-tubulin levels in HUVECs or HASMCs, respectively.

2.11. Statistical analysis

Data were expressed as means ± SD values. The Student's *t*-test (2-tailed p-values) or Mann-Whitney test was used for comparing variables that were either normally or not normally distributed, respectively, in two groups. Otherwise, statistical significance was determined using ANOVA, followed by the Kruskal-Wallis test. Values less than 0.05 were deemed to correspond to differences between means of two independent experiments that are statistically significant. A p-value of <0.05 was considered to be statistically significant, wherein $^{*}p < 0.05$, $^{**}p < 0.01$, and $^{***}p < 0.001$. GraphPad Prism 6 was used to determine the statistical significance.

3. Results

3.1. IS treatment-induced senescence in HUVECs

HUVECs treated with IS were characterized by a significant increase in senescence-associated β-galactosidase (SA-β-gal) stained cells, as compared to that in control cells. IS-treated senescent cells underwent a change in the cell morphology and adopted a typical flattened and enlarged morphology (Fig. 2A). The percentage of senescent cells was determined by testing the SA-β-gal activity. The number of SA-β-gal-positive (senescent) cells was significantly increased in IS-treated HUVECs. Strikingly, although all IS exposure experiments were performed under the same conditions, the percentage of positive cells was diverse. As a consequence of this variation and based on previous studies (Alique *et al*., 2019), two distinct and significant groups with different senescence percentages emerged: one group had an intermediate or medium percentage of senescent cells (42.85 ± 4.72%), while the other had an elevated or high percentage of senescent cells (72.90 ± 13.09%), as compared to the percentage of non-treated endothelial cells (7.07 ± 2.87%) (Fig. 2B). The senescent phenotype was more characteristically present in the group exhibiting higher senescence levels than in the group exhibiting intermediate levels of senescence. The criterium applied to divide into 2 groups was based on a previous study (Alique *et al*., 2019) in an endothelial replicative senescence, a senescence-associated secretory phenotype (SASP) where endothelial cells achieved up to 69% (69.36 ± 1 1.30%) of senescence, similar to the IS-treated group called with a elevated or high percentage of senescent cells (72.90 ± 13.09%), a stress-induced premature senescence (SIPS). The second IS-treated group is defined as intermediate or medium percentage of senescent cells associated with a percentage of 42.85 ± 4.72% and presents a lower percentage of senescence compared with endothelial replicative senescence as previously reported (Alique *et al*., 2019).

To confirm the senescent phenotype, protein senescence markers were tested. Cyclin D1 and Lamin B1 protein levels were measured via Western blot analysis. When the senescence levels were intermediate or elevated, IS-treated endothelial cells showed Lamin B1 downregulation, as compared to control endothelial cells (Fig. 2C and 2D). Whereas, Cyclin D1 levels were only significantly decreased during the IS-induced elevation in senescence levels. Thus, these data confirm that cells treated with IS for 3 days generated senescent endothelial cells, which validates our model *in vitro*.

3.2. MicroRNA expression in IS-treated HUVECs

Next, we studied about how microRNAs were implicated in endothelial damage, resulting in the senescent phenotype, as a consequence of changes introduced in endothelial cells via the stimulus provided by IS treatment. Therefore, the expression levels of miR-126 (3p and 5p), miR-21 (3p and 5p), miR-155, miR-210, miR-125b, miR-150, miR-1915, miR-601, and miR-575 in HUVECs have been analyzed in this study (Fig. 3). The results showed that the number of both types of miR-126 strands decreased among the endothelial cells exhibiting IS-induced elevated percentages of senescence. In the case of miR-21, only miR-21-3p was downregulated in IS-induced elevated senescence in cells, while the strand miR-21-5p was not modified. MiR-155 levels were also

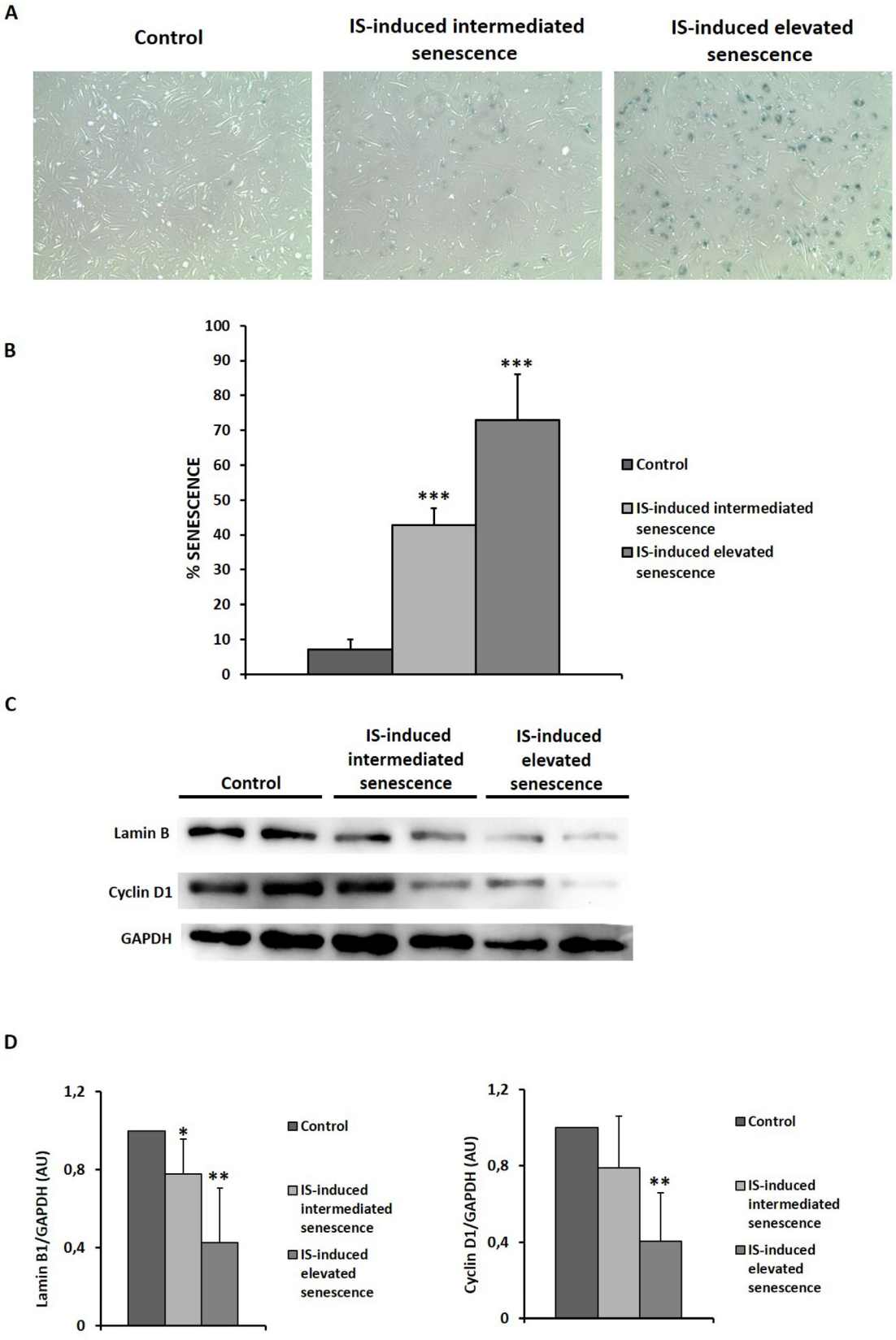

Fig. 2. Senescence in HUVECs. HUVECs develop a senescence phenotype after IS treatment (250 μM; 3 days). The percentage of senescent HUVECs was determined by senescence-associated β-galactosidase staining. (A) Phase-contrast microscopy pictures. (B) The data represent means ± SD and are expressed as a percentage of total cells and fold induction, with regard to control values. Control (n = 6); IS-induced intermediate senescence (n = 4); IS-induced elevated senescence (n = 4); 8 random fields each; magnification, x100. (C) Lamin B1 and Cyclin D1 representative Western blots under different conditions. After probing with GAPDH, it was confirmed that equal amounts of proteins were loaded. (D) The graphs show that densitometric band analysis levels were normalized to GAPDH levels in arbitrary units (AU). In B and D, data represent means ± SD values and are expressed as the fold induction, as compared to control values. Control (n = 6); IS-induced intermediate senescence (n = 4); IS-induced elevated senescence (n = 4). *$p < 0.05$, **$p < 0.01$, and ***$p < 0.001$. Control HUVECs *vs.* IS-treated HUVECs.

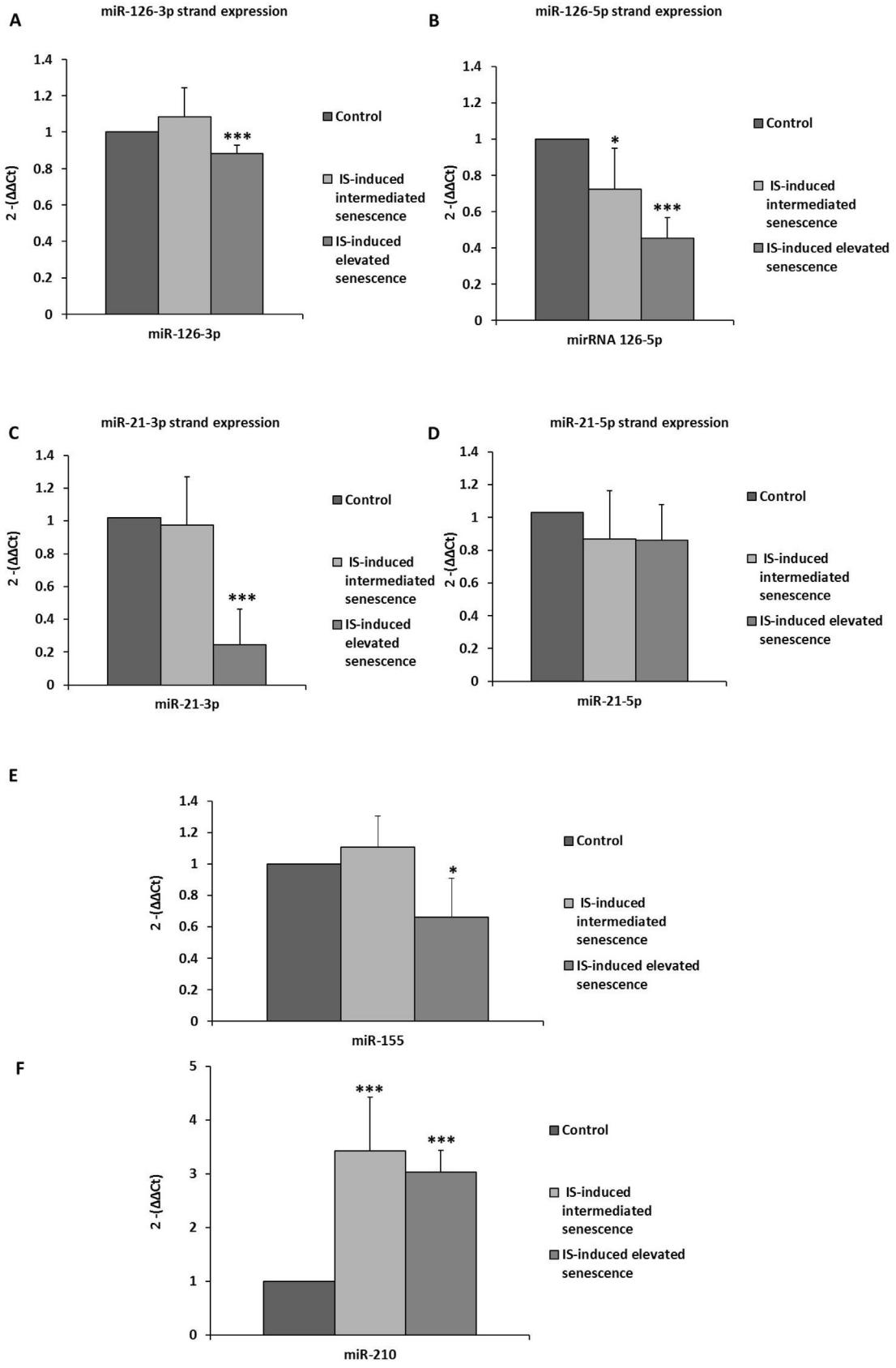

Fig. 3. miRNAs in IS-treated HUVECs. qPCR analysis of miR-126-3p (A), miR-126-5p (B), miR-21-3p (C), miR-21-5p (D), miR-155 (E), and miR-210 (F) was performed in control and IS-treated endothelial cells using the ΔCt method; U6 snRNA was used for normalization in HUVECs. *p < 0.05 and ***p < 0.001 for Control *vs.* IS-induced intermediate senescence. Control (n = 6); IS-induced intermediate senescence (n = 4); IS-induced elevated senescence (n = 4).

diminished in the group exhibiting an elevated rate of senescence, and only miR-210 levels were increased in both groups of senescent HUVECs. These miRNAs were involved in endothelial homeostasis and regulated by IS treatment.

Moreover, we have also measured the levels of some miRNAs associated with endothelial cell damage caused by IS treatment [20]. However, there were no changes in the levels of miR-125b, miR-150, miR-1915, miR-601, and miR-575 in IS-induced senescence groups, with regard to the control (Fig. 1S); consequently, they did not appear to be involved in the damage caused by IS in endothelial cells.

3.3. MVs released and annexin A5 expression

We have also determined the number of MVs in IS-treated and control HUVECs. The number of HUVEC-derived MVs was assessed by flow cytometry (number/μL), and the number of endothelial cells was measured using the Neubauer chamber. Annexin A5, a phosphatidylserine (PS) binding protein, is commonly used to characterize MVs, and during MVs formation, the presence of PS is confined to the exoplasmic membrane leaflet and exposed in the MV surface. A representative analysis is shown in Fig. 4 (A-D) The ratio was expressed as the fraction between the MVs number/HUVECs number (MVs per cell ratio). Remarkably, a significant ($p < 0.001$) increase in the production of MVs per cell was observed during IS-induced elevated senescence (9.92 ± 4.29, n = 4), as compared to the control (1.68 ± 1.00, n = 6); an insignificant increase (2.88 ± 1.17, n = 4) was also observed in the IS-induced intermediate senescence group (Fig. 4E).

Thus, besides the MVs per cell ratio, we have studied PS exposure in the MVs. No changes were detected in annexin A5 expression by flow cytometry (expressed by mean fluorescence intensity; MFI) in the control and IS-treated HUVEC MVs (Fig. 2S).

3.4. MVs from IS-induced elevated senescent endothelial cells contain calcium

Following the characterization of MVs, scanning electron microscopy-energy dispersive X-ray spectroscopy (SEM-EDX) was performed to detect whether MVs contained calcium or other ions. EDX elemental analysis revealed that the mean calcium content in MVs from IS-treated endothelial cells, determined from several regions in each sample, was 12-fold more than that of MVs from untreated endothelial cells (Table 1). Besides, IS-treated HUVECs-derived MVs contain higher levels of magnesium than control HUVECs, and no changes were detected for other ions, such as phosphorus and potassium. Moreover, the calcium content in MVs was measured with a SEM-mapping micrograph, which showed that calcium was homogeneously distributed into MVs from control and IS-treated endothelial cells.

3.5. MVs released from IS-treated HUVECs induced calcification in HASMCs

To evaluate the possibility that MVs from IS-treated HUVECs resulted in calcification, human aortic smooth muscle cells (HASMCs) were cultured in the presence of MVs (50,000 MVs/mL) from control and IS-treated HUVECs for 9, 20, and 30 days. In HASMCs, calcium deposits were evaluated using alizarin red on different days (Fig. 5 and Fig. 3S). MVs from both groups of IS-treated endothelial cells induced calcification after 30 days of treatment, notably in MVs from IS-induced elevated senescence. Calcium deposits were not observed in HASMCs with MVs from control endothelial cells. HASMCs were also incubated with phosphate, to induce a calcification condition, as a positive control; in the negative control, HASMCs were grown without MVs. To confirm these findings, the calcium content was quantified using a colorimetric method based on phenolsulfonephthalein reagent, 30 days after the presence of MVs was observed (Fig. 5B). Calcium accumulation caused by MVs from IS-treated HUVECs was significantly increased in HASMCs on day 30, as compared to HASMCs without MVs. Significant differences were also observed in the development of calcification on day 30, between both groups of MVs obtained from IS-treated HUVECs (Fig. 5B).

3.6. MVs from IS-treated HUVECs increased pro-calcification genes in HASMCs

The expression of pro-calcifying genes in HASMCs was analyzed by qPCR. The results demonstrated that MVs from both groups of IS-treated endothelial cells induced Runx2 and BMP2 expression, via two essential procalcifying genes (Fig. 6A). Concretely, MVs from IS-induced intermediate senescent cells increased Runx2 gene levels in HASMCs over the longest treatment duration (30 days), whereas BMP2 gene expression was augmented 20 and 30 days after MV treatment. However, for MVs obtained from IS-induced elevated levels of senescent cells, Runx2 gene levels were elevated after 9, 20, and 30 days, and BMP2 levels were increased after 20 and 30 days of treatment.

To corroborate the procalcifying vascular phenotype, the expression of a specific HAMSCs marker (SM22α) was evaluated. Western blot assays established that SM22α levels were diminished in HASMCs after treatment with MVs from IS-treated HUVECs on day 20 and 30 (Fig. 6B).

3.7. MVs released from IS-treated HUVECs modulated inflammatory genes in HASMCs

To elucidate the effect of the inflammation on the progression of calcification, we performed qPCR analysis for genes expressing different pro-inflammatory cytokines (TNF-α, TWEAK, CCL2, CCL5, and IL-6) that were implicated in the calcification process in HASMCs.

Our results showed that TWEAK (cytokine tumour necrosis factor-like weak inducer of apoptosis) mRNA levels were decreased in HASMCs treated with MVs from IS-treated endothelial cells on day 20 and 30 (Fig. 7A). However, TNF-α caused a significant increase in the number of HASMCs treated with MVs obtained from the IS-induced intermediate senescence group and a significant decrease in the IS-induced group exhibiting elevated senescence (Fig. 7). Furthermore, other inflammatory mediators, such as CCL2 and CCL5 were also evaluated. The chemokine mRNA levels of both these mediators increased significantly in HASMCs after treatment with MVs from the cells exhibiting IS-induced intermediate senescence; however, no changes were observed in the elevated senescence group (Fig. 7B and C). Finally, we evaluated the expression of IL-6, a cytokine linked with chronic inflammation. The results showed that IL-6 gene expression levels were significantly reduced in MVs-treated cells on day 20, whereas it was significantly overexpressed in cells treated with both groups of MVs on day 30 (Fig. 7E).

4. Discussion

VC is characteristically observed in CKD, and is associated with the damage induced by uremic toxins and other substances in vascular cells [2]. The identification of VC in CKD patients seems to be critical to prevent the progression of CVD, which is a principal cause of morbi-mortality in these patients. Moreover, some studies resported that some uremic toxins, such us IS and p-cresyl sulfate, trigger calcification in vessels throught endothelial dysfunction of

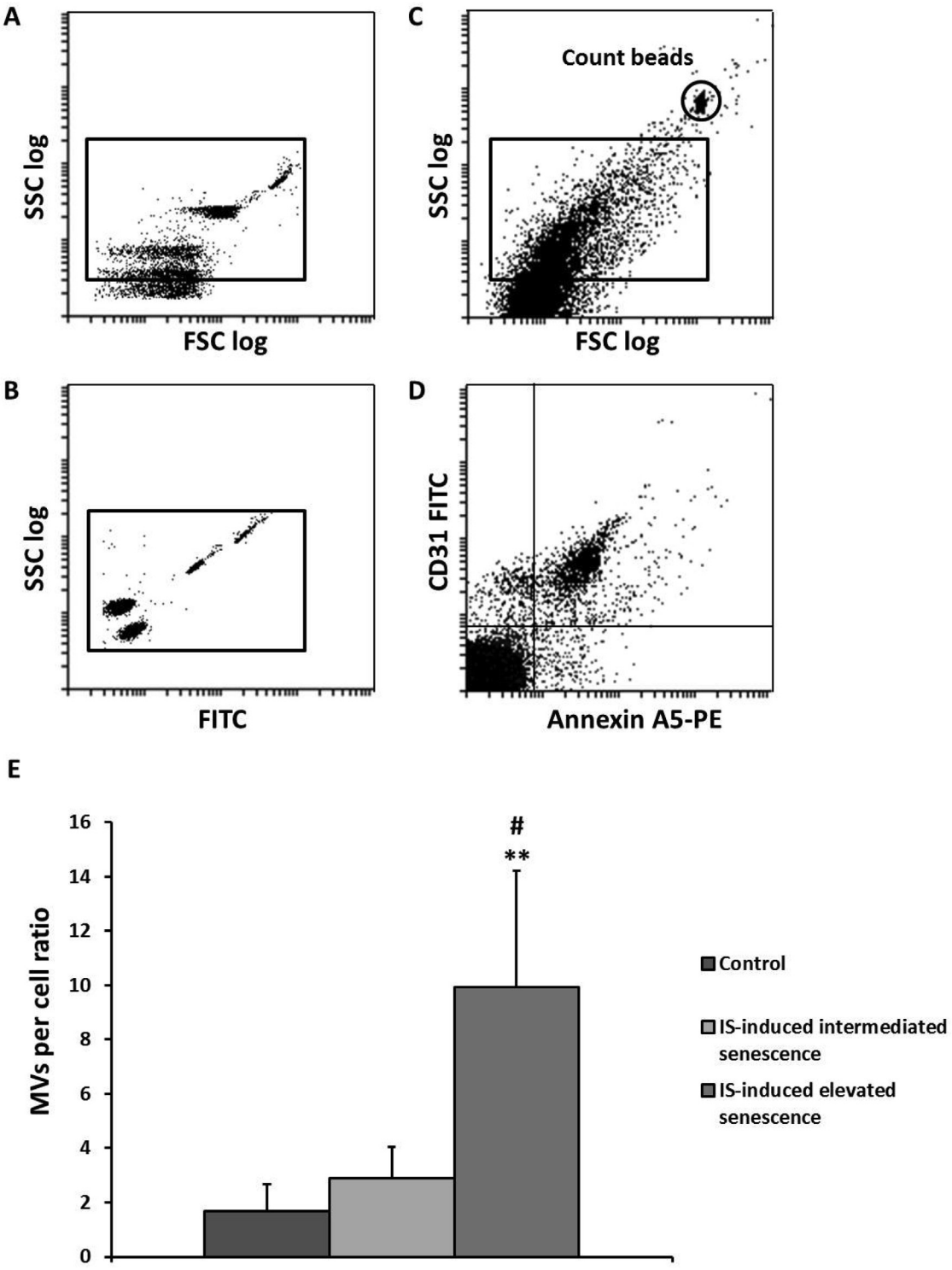

Fig. 4. Characterization and measurement (MVs per cell ratio) of MVs generated by IS treatment in HUVECs. Representative graphs showing the results of flow cytometry analysis of MVs (A-D). Fluorescence-gated beads with sizes between 0.22 μm and 1.35 μm were used for determining gates(A,B). MVs were plotted using an FSC logarithmic (FS log)/SSC logarithmic (SS log) dot-plot histogram and were gated in the window selected above; it was necessary to use bead counts in each experiment, to calculate the concentration of MVs per unit volume of the sample (C). Size-selected MVs are plotted as a function of their double fluorescence for specific Annexin A5-PE binding and CD31-FITC (D). (E) The number of HUVEC-derived MVs was assessed by flow cytometry, and the number of endothelial cells was measured using the Neubauer chamber. The ratio was expressed as the fraction of MVs number/HUVECs number in each experiment (MVs per cell ratio). Control (n = 6); IS-induced intermediate senescence (n = 4); IS-induced elevated senescence (n = 4). **p < 0.01, control HUVECs *vs.* IS-induced elevated senescence. #p < 0.001, IS-induced intermediate senescence *vs.* IS-induced elevated senescence.

CKD rats [29–31]. Nowadays, there is no diagnostic method to evaluate the initial steps during VC formation and CKD patients at risk of developing VC, and this pathology is detected when the process is irreversible [2].

Recently, different studies have supported the role of MVs produced by many cells that promote VC [32–34], which shows that MVs have novel roles in VC, although their potential use as VC biomarkers is still unknown. Some reports have demonstrated that

Table 1
EDX analysis of control and MVs from IS-treated elevated senescent cells. The relative percentage of ion content in MVs obtained from control and IS-treated HUVECs. Control (n = 4); elevated senescence group (n = 4). *p < 0.05 and ***p < 0.001, ns: not significant. Control HUVEC MVs *vs.* elevated senescent HUVEC MVs.

Relative percentage (%)	Control MVs (Mean ± SD)	IS-induced elevated senescence (Mean ± SD)	p-value
Calcium	0.495 ± 0.439	6.020 ± 1.762	***(0.001)
Magnesium	0.178 ± 0.022	0.583 ± 0.324	*(0.047)
Phosphorus	1.050 ± 0.501	1.440 ± 0.616	ns
Potassium	6.460 ± 1.914	6.217 ± 1.452	ns

plasma endothelial MVs are potential diagnostic and prognostic biomarkers in patients with CVD [3,35,36]. However, the clinical application of the MVs for the prognosis of disease could have some limitations, due to the origin of cells that produce MVs. It has been reported that the measurement of specific MVs from each kind of cell is essential for characterizing specific surface markers [37]. The results of this study extend the use of endothelial MVs to identified CKD patients at risk of developing VC. Besides, the fact that endothelial MVs released from endothelial cells undergo IS-induced senescence and promote calcification in VSMCs might offer new perspectives that would enable the development of therapies based on the modification of the procalcifying actions of these MVs.

Uremic toxins promote endothelial dysfunction in CKD patients. Accumulating pieces of evidence support the fact that among other cells, endothelial cells undergo premature senescence induced by uremic toxins [38–40]. IS treatment restrains the number of cell divisions that occur and cause endothelial cells to achieve SIPS, which is characterized by an irreversible arrest in the cell cycle [41]. SIPS is a physiopathological CVD mechanism associated with CKD [42]. In our *in vitro* model, an increasing percentage of senescent cells have been observed in the endothelial cells throughout the process of culturing of cells with IS. This uremic toxin generates premature endothelial senescence in different proportions, thus highlighting the susceptibility of the endothelial cells in primary culture, because of their limited lifespan. Perhaps, the results highlighted the sensitivity of primary culture cells of IS-treated HUVECs. Because primary cells are derived from tissue and not modified, they are more similar to the *in vivo* state and exhibit a normal physiology.

Moreover, primary endothelial cells have a limited lifespan, and IS treatment abrogates cellular division; cells become senescent in an experiment-dependent fashion. Notably, the expression of Cyclin D1, a protein that played a critical role in the cell cycle and whose levels are reportedly elevated during senescence process [43], was diminished in IS-induced elevated senescent cells. This data indicated that this type of senescence might have occurred in the endothelium; in this case, SIPS could be induced by IS, and regulate the proteins involved in the cell cycle and, therefore, in senescence (SASP and SIPS).

Recent studies have shown that miRNAs are critical modulators of endothelial homeostasis due to their role in controlling endothelial cell functions and, therefore, are implicated in vascular dysfunction [44]. miRNAs have been associated with some chronic and irreversible pathologies, such as atherosclerosis [44,45] and in CKD-associated CVD [46]. We have observed that IS treatment modifies the expression of some miRNAs in HUVECs; in particular, miR-126, miR-21-3p, and miR-210 levels are altered in cells treated with IS; more precisely, the levels of both strands of miR-126 were decreased in IS-treated endothelial cells, and the modulation was associated with the senescence percentage in endothelial cells. MiR-126 is an essential miRNA involved in homeostasis and senescence in endothelial cells [43,47], and is associated with endothelial shear stress [44]. Furthermore, miR-210 plays a critical role in the vasculature due to mediated angiogenesis in endothelial cells [48]. In general, miR-126, miR-21-3p, and miR-210 are associated with endothelial functions and are modulated by IS, which indicates that this toxin induced changes in the miRNA content of MVs, and could be involved in the development of pathologies in the vasculature and therefore contribute to the development of CKD-associated CVD.

Besides, endothelial cells damaged by the uremic toxin IS produced a large amount of MVs. Our results showed that the release of MVs was incremented in IS-treated endothelial cells and was perhaps associated with the percentage of senescent endothelial cells. With regard to the delivery of MVs from endothelial cells, some studies showed that damaged endothelial cells release an increased number of MVs [5,6], which confirms our data obtained using IS treatment. This data represents an advantage in identifying CKD patients with an endothelial injury.

Recently, our group has reported about how senescent endothelial cells produce MVs that trigger the development of VC [10]. Another useful hint to confirm this intriguing question is that the induction of premature senescence by uremic toxins, a pathological mechanism in CVD associated with CKD, generate MVs which could modify VSMCs. Our experimental approach is based on vascular cells exposure to MVs from IS-treated endothelial cells, these MVs have a high content of calcium (up to 12 times more of calcium than MVs from control endothelial cells) and could increase the VSMC susceptibility to bone transformation and, therefore, could promote VC. Our previous results demonstrated that MVs delivery from a model of replicative endothelial senescence (SASP) was able to produce calcium accumulation in VSMCs at day 9 [10]. The present results confirmed the fact that MVs from damaged HUVECs caused a progressive level of calcium accumulation in VSMCs, which was maximized at day 30. These data confirm that the effect of endothelial MVs on premature senescence in CKD patients causes VC, in the same manner as that observed during physiological aging (replicative senescence model *in vitro*); however, both processes presented differences with regard to VC development. Remarkably, during replicative endothelial senescence (SASP), generated MVs caused VC for shorter durations, while during IS-induced senescence in endothelial cells, the release of MVs caused VC for longer durations. Even though VC development is the final step in both cases, calcium accumulation in MVs of senescent endothelial cells occurs in a different manner, because the time points at which calcium deposits appear are different and depend on the type of senescence, i.e. SIPS or SASP. During SASP, endothelial MVs caused VC for shorter durations, while during SIPS, MVs released by damaged endothelial cells caused VC for longer durations. Thereby, endothelial MVs in vascular vessels might not all be equal in number, and specific MVs present prior to and during the VC process might have been targeted, to prevent the pathology from appearing in CKD patients. These results elucidate a common mechanism underlying premature aging and age-associated VC, and differences in the timeline during which MVs caused VC to develop were identified, depending on the kind of senescence induced by the stimulus (IS) or physiology. Recently, Panfoli et al. [49] described MVs as promising biological tools for diagnosis and therapy. The targeting of specific MVs in the beginning of the developmental period and during the late stages of VC might be useful for preventing the pathology from appearing in CKD patients.

Increasing evidence has shown that endothelial inflammation and senescence significantly contribute to multiple vascular diseases, including atherosclerosis [47]; in fact, the injury of the endothelium provokes the release of some mediators that act as pro-inflammatory cytokines [39,40]. The results of our study have demonstrated that pro-inflammatory cytokines mediate the development of VC. Previous results showed that senescence is a

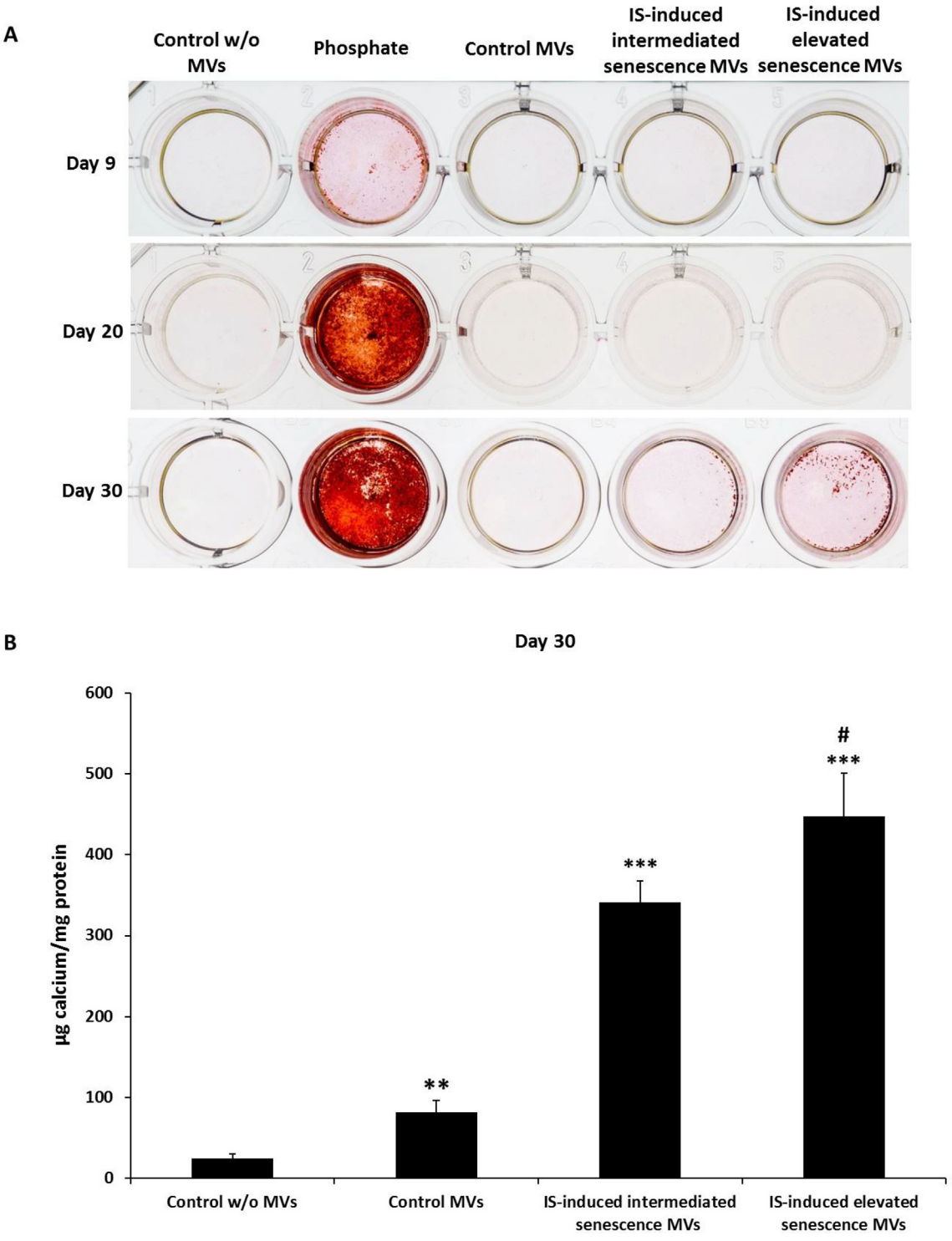

Fig. 5. Induction of calcification in HASMCs. HASMCs were cultivated with 50,000 MVs/mL from the control and IS-treated HUVECs for a different number of days. (A) Qualitative calcification was performed by staining cells with alizarin red. A representative from five different experiments is shown. (B) Calcium content was determined by spectrophotometry using phenolsulphonphthalein dye after 30 days of treatment. The graphs present the calcium content of the cells, expressed as µg/mg protein. The data represent the means ± SD of 3 independent experiments. **p < 0.05 *vs.* control w/o MVs; *** p < 0.001 *vs.* control w/o MVs, and # p < 0.001 *vs.* IS-induced intermediate senescence MVs at the same time.

phenomenon characterized by chronic inflammation and, therefore, by the release of pro-inflammatory factors [50]. We have tested the expression of cytokines associated with the pro-calcification process, to demonstrate that TWEAK, a member of the tumor necrosis factor (TNF) superfamily, recently described as a biomarker of CVD and directly implied in osteogenic transition [51], and TNF-α -which enhances calcification [52], were modulated in HASMCs with MVs of IS-treated endothelial cells. TWEAK can regulate cell proliferation, migration, differentiation, death, inflammation, fibrosis, and angiogenesis [53–56]; it has a synergic effect *in vitro* on the promotion of mineralization (osteogenic transition) induced by inorganic phosphate in HAMSCs [51]. We have

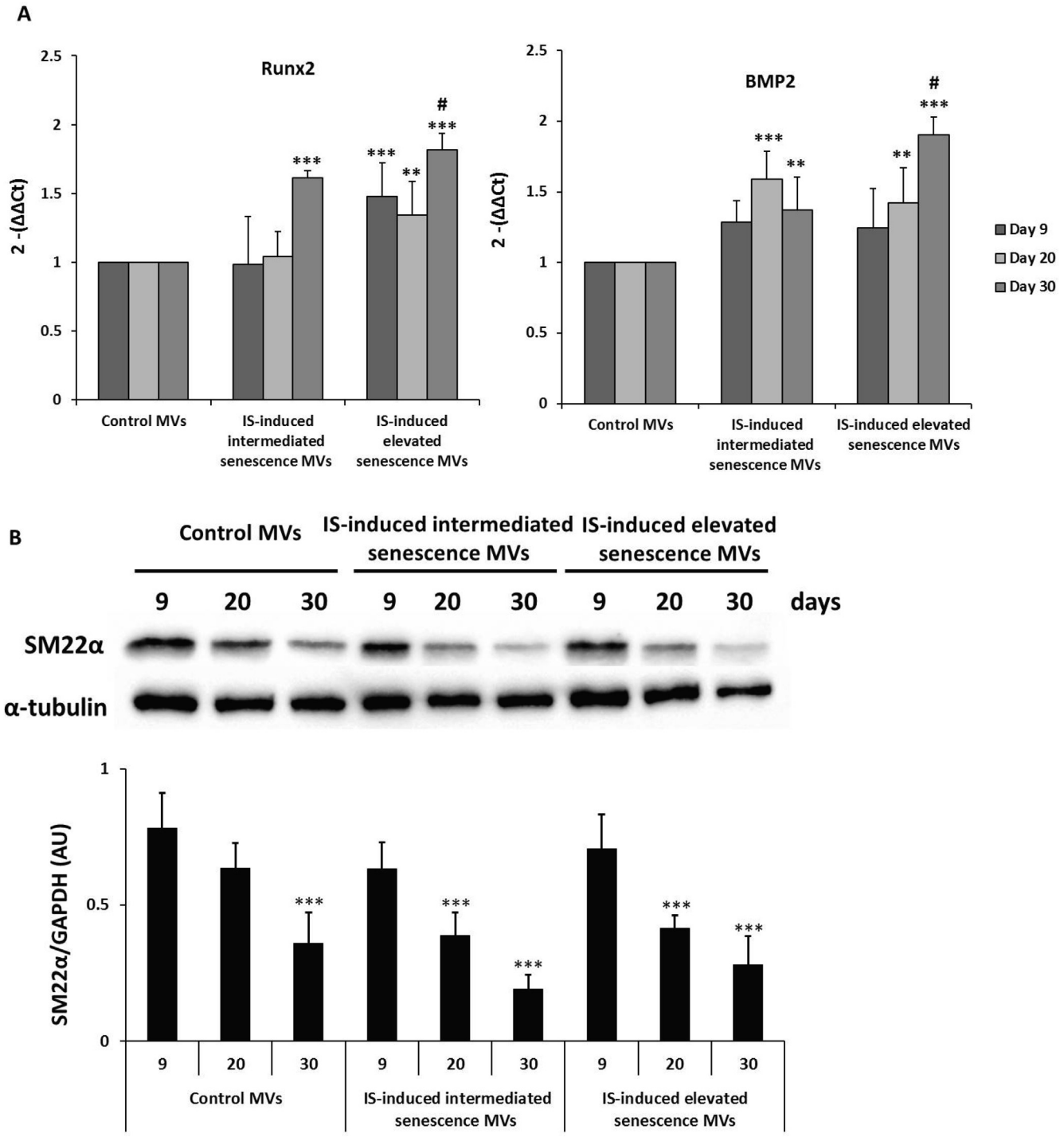

Fig. 6. HASMCs calcification markers. (A) qPCR analysis of Runx2 and BMP2 mRNA obtained from MVs-treated HASMCs using the ΔCt method. HPRT1 mRNA was used for normalization. n = 2 per duplicate. **p < 0.05 *vs.* control MVs; ***p < 0.001 *vs.* control MVs; #p < 0.05 *vs.* IS-induced intermediate senescence MVs at the same time. (B) Western blot analysis of SM22α from MVs-treated HASMCs was performed for different days. Equal protein loading was confirmed after probing with α-tubulin. The graph presents data regarding densitometric bands analysis normalized to α-tubulin in terms of arbitrary units (AU). n = 2 per duplicate. ***p < 0.001 *vs.* 9 days at the same time.

also focused on studying CCL2 and CCL5, which play a critical role in atherogenesis and the development of VC [57,58]. As in the case of the previous cytokines, the gene expression of both these molecules was increased in HASMCs after incubation with MVs from IS-treated HUVECs (intermediate senescence). Arterial inflammation is common in patients with diabetes mellitus and CKD, and is associated with increased levels of TNF-α. Moreover, TNF-α induces the generation of osteogenic BMP-2 mRNA and leads to increased aortic calcium accumulation [59]. Finally, IL-6 gene expression was evaluated, due to its direct implication in the inflammation process and the calcium deposits in VSMCs [60]. Our results showed that the IL-6 gene was overexpressed in HASMCs treated with MVs from IS-treated endothelial cells. Furthermore, it has been reported that because of ongoing inflammation, additional calcium-phosphate crystals are formed, which might get aggregated [61]. Altogether, the measurement of pro-inflammatory gene expression

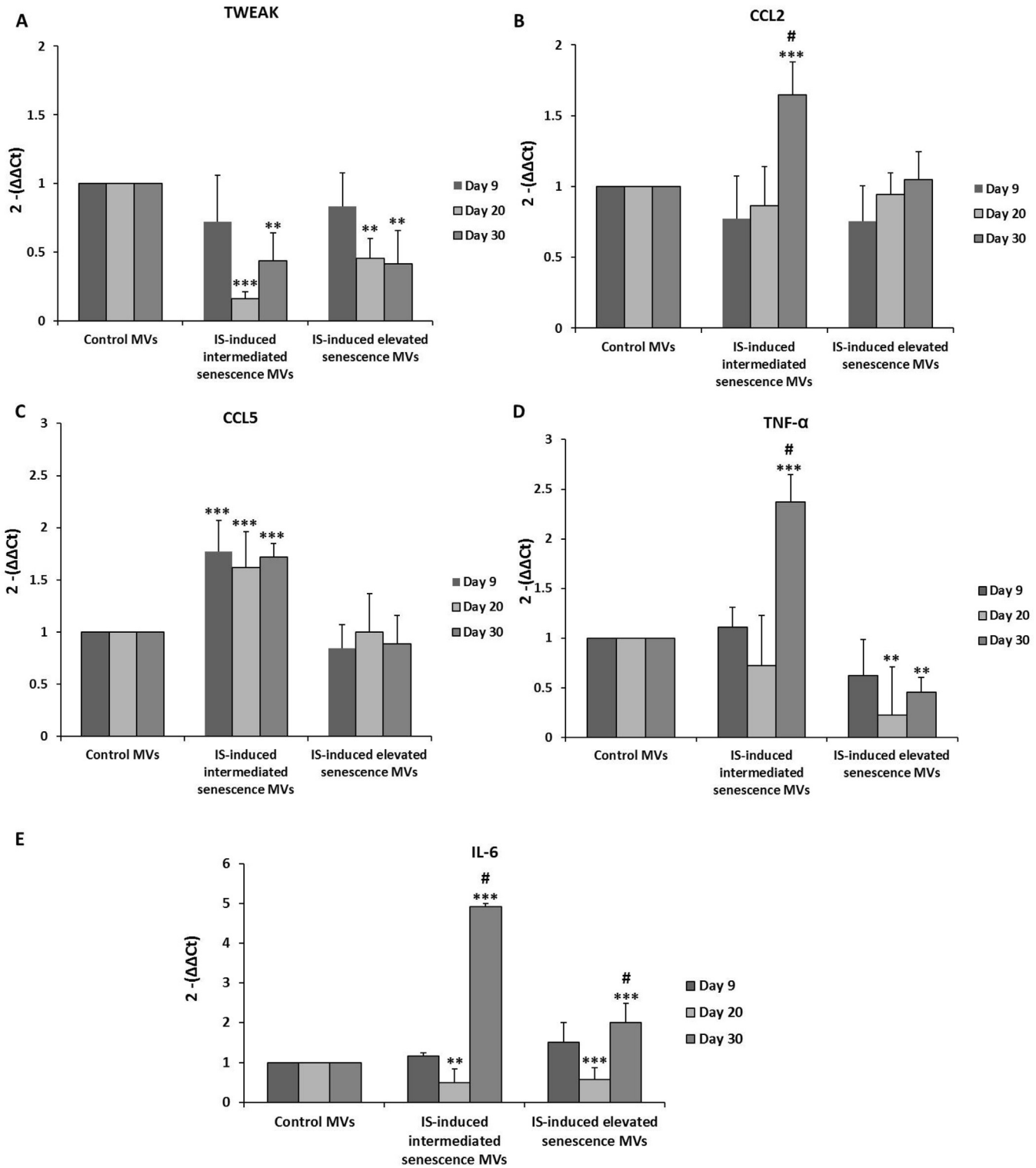

Fig. 7. Effect of MVs on pro-inflammatory genes in HASMCs. qPCR analysis of inflammatory mRNAs in HASMCs treated with control MVs and IS-treated HUVECs using the ΔCt method; HPRT1 mRNA was used for normalization. n = 2 per duplicate. **p < 0.05 *vs*. control MVs; ***p < 0.001 *vs*. control MVs; #p < 0.05 *vs*. MVs obtained simultaneously from IS-induced intermediate senescent cells.

in HASMCs after incubation with MVs from IS-treated endothelial cells confirms that MVs released by IS-damaged endothelial cells generate an inflammatory response in HASMCs, which could trigger VC development. In this sense, the inhibition of the inflammatory activity of VSMCs induced by endothelial MVs might be a potential therapeutic target that can prevent vascular calcification in CKD patients. Curiously, treatment with control MVs in HASMCs caused calcium deposits after 30 days, probably due to cellular changes caused by the presence of MVs alone. These results confirm the fact that the inflammatory process is a condition associated with osteogenesis in the vasculature and that MVs from damaged endothelial cells modulate the inflammatory process in VSMCs. The presence of some cytokines in endothelial MVs might provide prognostic information about the process of VC by MVs.

5. Conclusions

The uremic toxin IS generates stress in endothelial cells and induces premature senescence and an increase in the release of MVs that promote the development of VC. Our *in vitro* experimental design has shown for the first time that these MVs represent a new VC mediator in the osteogenic transition mechanism in vascular smooth muscle cells. Finally, this study also demonstrates the that MVs are involved in the inflammatory response of vascular smooth muscle cells prior to VC development. These results might be useful in the development of biomarkers and therapeutic tools for preventing or treating patients with CVD and/or CKD at risk of developing VC. Although these data need to be confirmed by performing clinical studies, the results obtained actively support the fact that plasma endothelial MVs could be used to identify CKD patients at risk of developing VC and offer new perspectives for achieving progress in future therapies designed to modulate the altered activity of EVs. Further investigations on MVs are required for using this information for the development of clinical applications.

Acknowledgments

This study has been funded by Instituto de Salud Carlos III through the project "PI17/01029" and "PI19/00240" (co-funded by European Regional Development Fund "A way to make Europe"), Santander/UCM, under grant PR41/17-20964, and Sociedad Española de Nefrologia and "Proyectos de Investigación del Programa Propio de la UAH," under grants UAH-GP2018-4 and CCG2018/BIO-010, respectively. We are grateful to Lourdes Bohorquez for her technical assistance.

Disclosure of interest

The authors state that they have no conflicts of interest to declare.

Appendix A. Supplementary data

Supplementary data to this article can be found online at https://doi.org/10.1016/j.csbj.2020.04.006.

References

[1] Goligorsky MS. Pathogenesis of endothelial cell dysfunction in chronic kidney disease: a retrospective and what the future may hold. Kidney Res Clin Pract 2015;34(2):76–82. PubMed PMID: 26484026. PMCID: PMC4570605. Epub 2015/06/04.eng..

[2] Soriano S, Carmona A, Triviño F, Rodriguez M, Alvarez-Benito M, Martín-Malo A, et al. Endothelial damage and vascular calcification in patients with chronic kidney disease. Am J Physiol Renal Physiol 2014;307(11). F1302-11. PubMed PMID: 25339701. Epub 2014/10/22.eng.

[3] Jansen F, Li Q, Pfeifer A, Werner N. Endothelial- and immune cell-derived extracellular vesicles in the regulation of cardiovascular health and disease. JACC Basic Transl Sci 2017;2(6):790–807. PubMed PMID: 30062186. PMCID: PMC6059011. Epub 2017/12/25.eng..

[4] Yáñez-Mó M, Siljander PR, Andreu Z, Zavec AB, Borràs FE, Buzas EI, et al. Biological properties of extracellular vesicles and their physiological functions. J Extracell Vesicles 2015;4:27066. PubMed PMID: 25979354. PMCID: PMC4433489.eng..

[5] Larson MC, Hillery CA, Hogg N. Circulating membrane-derived microvesicles in redox biology. Free Radic Biol Med 2014;73:214–28. PubMed PMID: 24751526. PMCID: PMC4465756. Epub 2014/04/18.eng.

[6] França CN, Izar MC, Amaral JB, Tegani DM, Fonseca FA. Microparticles as potential biomarkers of cardiovascular disease. Arq Bras Cardiol. 2015 Feb;104 (2):169-74. PubMed PMID: 25626759. PMCID: PMC4375661. Epub 2015/01/27. eng|por.

[7] Bodega G, Alique M, Puebla L, Carracedo J, Ramírez RM. Microvesicles: ROS scavengers and ROS producers. J Extracellular Vesicles 2019;8(1):1626654. PMCID: PMC6586107. Epub 2019/06/17.eng..

[8] Liu M-L, Williams KJ. Microvesicles: potential markers and mediators of endothelial dysfunction. Current Opin Endocrinol Diabetes Obesity 2012;19 (2):121–7. PubMed PMID: 22248645. PMCID: PMC5031554.eng..

[9] McVey MJ, Kuebler WM. Extracellular vesicles: biomarkers and regulators of vascular function during extracorporeal circulation. Oncotarget 2018;9(98). PubMed PMID: 30647856. PMCID: PMC6324688. Epub 2018/12/14. eng.

[10] Alique M, Ruíz-Torres María P, Bodega G, Noci MaríaV, Troyano N, Bohórquez L, et al. Microvesicles from the plasma of elderly subjects and from senescent endothelial cells promote vascular calcification. Aging 2017;9(3):778–89. PubMed PMID: 28278131. PMCID: PMC5391231.eng.

[11] Carracedo J, Alique M, Ramirez-Carracedo R, Bodega G, Ramirez R. Endothelial extracellular vesicles produced by senescent cells: pathophysiological role in the cardiovascular disease associated with all types of diabetes mellitus. Curr Vasc Pharmacol 2018. PubMed PMID: 30124156. Epub 2018/08/19.eng.

[12] Alique M, Ramírez-Carracedo R, Bodega G, Carracedo J, Ramírez R. Senescent microvesicles: A novel advance in molecular mechanisms of atherosclerotic calcification. Int J Mol Sci 2018;19(7). PubMed PMID: 29987251. PMCID: PMC6073566. Epub 2018/07/09.eng..

[13] Lei Q, Liu T, Gao F, Xie H, Sun L, Zhao A, et al. Microvesicles as potential biomarkers for the identification of senescence in human mesenchymal stem cells. Theranostics 2017;7(10):2673–89. PubMed PMID: 28819455. PMCID: PMC5558561. Epub 2017/07/06. eng..

[14] Schurgers LJ, Akbulut AC, Kaczor DM, Halder M, Koenen RR, Kramann R. Initiation and propagation of vascular calcification is regulated by a concert of platelet- and smooth muscle cell-derived extracellular vesicles. Front Cardiovasc Med 2018;5(36). PubMed PMID: 29682509. PMCID: PMC5897433. Epub 2018/04/06.eng..

[15] Vajen T, Benedikter BJ, Heinzmann ACA, Vasina EM, Henskens Y, Parsons M, et al. Platelet extracellular vesicles induce a pro-inflammatory smooth muscle cell phenotype. J Extracell Vesicles 2017;6(1):1322454. PubMed PMID: 28717419. PMCID: PMC5505004. Epub 2017/05/16. eng..

[16] Pan Q, Liu H, Zheng C, Zhao Y, Liao X, Wang Y, et al. Microvesicles Derived from Inflammation-Challenged Endothelial Cells Modulate Vascular Smooth Muscle Cell Functions. Front Physiol. 2016;7:692. PubMed PMID: 28127288. PMCID: PMC5226944. Epub 2017/01/12.eng.

[17] Khan SY, Awad EM, Oszwald A, Mayr M, Yin X, Waltenberger B, et al. Premature senescence of endothelial cells upon chronic exposure to TNFα can be prevented by N-acetyl cysteine and plumericin. Sci Rep. 2017 01;7:39501. PubMed PMID: 28045034. PMCID: PMC5206708. Epub 2017/01/03.eng.

[18] Carrecedo J-R-C-R, Alique M, Ramírez-Chamond R. Endothelial cell senescence in the pathogenesis of endothelial dysfunction. Intech 2018.

[19] Carracedo J, Buendía P, Merino A, Soriano S, Esquivias E, Martín-Malo A, et al. Cellular senescence determines endothelial cell damage induced by uremia. Exp Gerontol 2013;48(8):766–73.

[20] Carmona A, Agüera ML, Luna-Ruiz C, Buendía P, Calleros L, García-Jerez A, et al. Markers of endothelial damage in patients with chronic kidney disease on hemodialysis. Am J Physiol-Renal Physiol 2017;312(4):F673–81.

[21] Buendía P, Oca AM, Madueño JA, Merino A, Martín-Malo A, Aljama P, et al. Endothelial microparticles mediate inflammation-induced vascular calcification. FASEB J 2015;29(1):173–81.

[22] Wyatt CM, Drueke TB. Vascular calcification in chronic kidney disease: here to stay?. Kidney Int 2017;92(2):276–8.

[23] Raggi P. Coronary artery calcification predicts risk of CVD in patients with CKD. Nat Rev Nephrol 2017;13(6):324–6.

[24] Leopold JA. Vascular calcification: Mechanisms of vascular smooth muscle cell calcification. Trends Cardiovasc Med 2015;25(4):267–74.

[25] Robert S, Poncelet P, Lacroix R, Arnaud L, Giraudo L, Hauchard A, et al. Standardization of platelet-derived microparticle counting using calibrated beads and a Cytomics FC500 routine flow cytometer: a first step towards multicenter studies?. J Thromb Haemost 2009;7(1):190–7.

[26] Lötvall J, Hill AF, Hochberg F, Buzás EI, Di Vizio D, Gardiner C, et al. Minimal experimental requirements for definition of extracellular vesicles and their functions: a position statement from the International Society for Extracellular Vesicles. J Extracell Vesicles 2014;3(1):26913.

[27] Bodega G, Alique M, Bohórquez L, Ciordia S, Mena María C, Ramírez MR. The antioxidant machinery of young and senescent human umbilical vein endothelial cells and their microvesicles. Oxid Med Cell Longevity 2017;2017:1–12.

[28] Alkhatatbeh MJ, Enjeti AK, Baqar S, Ekinci EI, Liu D, Thorne RF, et al. Strategies for enumeration of circulating microvesicles on a conventional flow cytometer: Counting beads and scatter parameters. J Circul Biomarkers 2018;7.

[29] Opdebeeck B, D'Haese PC, Verhulst A. Molecular and Cellular Mechanisms that Induce Arterial Calcification by Indoxyl Sulfate and P-Cresyl Sulfate. Toxins (Basel). 2020 Jan;12(1). PubMed PMID: 31963891. PMCID: PMC7020422. Epub 2020/01/19.eng.

[30] Vanholder R, Schepers E, Pletinck A, Nagler EV, Glorieux G. The uremic toxicity of indoxyl sulfate and p-cresyl sulfate: a systematic review. JASN 2014;25 (9):1897–907.

[31] Hou YC, Liu WC, Zheng CM, Zheng JQ, Yen TH, Lu KC. Role of Vitamin D in Uremic Vascular Calcification. Biomed Res Int. 2017;2017:2803579. PubMed PMID: 28286758. PMCID: PMC5329659. Epub 2017/02/12.eng.

[32] Dusso A, Colombo MI, Shanahan CM. Not all vascular smooth muscle cell exosomes calcify equally in chronic kidney disease. Kidney Int 2018;93 (2):298–301.

[33] Viegas CSB, Santos L, Macedo AL, Matos AA, Silva AP, Neves PL, et al. Chronic Kidney Disease Circulating Calciprotein Particles and Extracellular Vesicles Promote Vascular Calcification: A Role for GRP (Gla-Rich Protein). Arterioscler Thromb Vasc Biol. 2018 03;38(3):575-87. PubMed PMID: 29301790. Epub 2018/01/04.eng.
[34] Bakhshian Nik A, Hutcheson JD, Aikawa E. Extracellular Vesicles As Mediators of Cardiovascular Calcification. Front Cardiovasc Med. 2017;4:78. PubMed PMID: 29322046. PMCID: PMC5732140. Epub 2017/12/11.eng.
[35] Dickhout A, Koenen RR. Extracellular vesicles as biomarkers in cardiovascular disease; chances and risks. Front Cardiovasc Med 2018;5(113).
[36] Chong SY, Lee CK, Huang C, Ou YH, Charles CJ, Richards AM, et al. Extracellular vesicles in cardiovascular diseases: alternative biomarker sources, therapeutic agents, and drug delivery carriers. Int J Mol Sci 2019;20(13):3272.
[37] Miller VM, Lahr BD, Bailey KR, Hodis HN, Mulvagh SL, Jayachandran M. Specific cell-derived microvesicles: Linking endothelial function to carotid artery intima-media thickness in low cardiovascular risk menopausal women. Atherosclerosis 2016;246:21–8.
[38] Wolley MJ, Hutchison CA. Large uremic toxins: an unsolved problem in end-stage kidney disease. Nephrol Dial Transplant 2018;33(suppl_3):iii6–iii11.
[39] Huang M, Wei R, Wang Y, Su T, Li P, Chen X. The uremic toxin hippurate promotes endothelial dysfunction via the activation of Drp1-mediated mitochondrial fission. Redox Biol 2018;06(16):303–13. PubMed PMID: 29573704. PMCID: PMC5953222. Epub 2018/03/16.eng.
[40] Saum K, Campos B, Celdran-Bonafonte D, Nayak L, Sangwung P, Thakar C, et al. Uremic Advanced Glycation End Products and Protein-Bound Solutes Induce Endothelial Dysfunction Through Suppression of Krüppel-Like Factor 2. JAHA 2018;7(1).
[41] Ott C, Jung T, Grune T, Höhn A. SIPS as a model to study age-related changes in proteolysis and aggregate formation. Mech Ageing Dev 2018;170:72–81.
[42] Dai L, Qureshi AR, Witasp A, Lindholm B, Stenvinkel P. Early Vascular Ageing and Cellular Senescence in Chronic Kidney Disease. Comput Struct Biotechnol J 2019;17:721–9.
[43] Alique M, Bodega G, Giannarelli C, Carracedo J, Ramírez R. MicroRNA-126 regulates Hypoxia-Inducible Factor-1α which inhibited migration, proliferation, and angiogenesis in replicative endothelial senescence. Sci Rep 2019;9(1).
[44] Fernández-Hernando C, Suárez Y. MicroRNAs in endothelial cell homeostasis and vascular disease:. Curr Opin Hematol 2018;25(3):227–36.
[45] Weber M, Baker MB, Moore JP, Searles CD. MiR-21 is induced in endothelial cells by shear stress and modulates apoptosis and eNOS activity. Biochem Biophys Res Commun 2010;393(4):643–8.
[46] Metzinger-Le Meuth V, Burtey S, Maitrias P, Massy ZA, Metzinger L. microRNAs in the pathophysiology of CKD-MBD: Biomarkers and innovative drugs. Biochimica et Biophysica Acta (BBA) - Molecular Basis of Disease 2017;1863(1):337–45.
[47] Qin B, Yang H, Xiao B. Role of microRNAs in endothelial inflammation and senescence. Mol Biol Rep 2012;39(4):4509–18.
[48] Chamorro-Jorganes A, Araldi E, Suárez Y. MicroRNAs as pharmacological targets in endothelial cell function and dysfunction. Pharmacol Res 2013;75:15–27.
[49] Panfoli I, Santucci L, Bruschi M, Petretto A, Calzia D, Ramenghi LA, et al. Microvesicles as promising biological tools for diagnosis and therapy. Expert Rev Proteomics 2018;15(10):801–8.
[50] Ventura MT, Casciaro M, Gangemi S, Buquicchio R. Immunosenescence in aging: between immune cells depletion and cytokines up-regulation. Clin Mol Allergy 2017;15(1).
[51] Hénaut L, Sanz AB, Martin-Sanchez D, Carrasco S, Villa-Bellosta R, Aldamiz-Echevarria G, et al. TWEAK favors phosphate-induced calcification of vascular smooth muscle cells through canonical and non-canonical activation of NFκB. Cell Death Dis 2016;7(7):e2305.
[52] Aghagolzadeh P, Bachtler M, Bijarnia R, Jackson C, Smith ER, Odermatt A, et al. Calcification of vascular smooth muscle cells is induced by secondary calciprotein particles and enhanced by tumor necrosis factor-α. Atherosclerosis 2016;251:404–14.
[53] Sanz AB, Sanchez-Niño MD, Izquierdo MC, Jakubowski A, Justo P, Blanco-Colio LM, et al. Tweak induces proliferation in renal tubular epithelium: a role in uninephrectomy induced renal hyperplasia. J Cell Mol Med 2009;13(9b):3329–42.
[54] Yoriki R, Akashi S, Sho M, Nomi T, Yamato I, Hotta K, et al. Therapeutic potential of the TWEAK/Fn14 pathway in intractable gastrointestinal cancer. Exp Ther Med 2011;2(1):103–8.
[55] Sanz AB, Justo P, Sanchez-Niño MD, Blanco-Colio LM, Winkles JA, Kreztler M, et al. The cytokine TWEAK modulates renal tubulointerstitial inflammation. JASN 2008;19(4):695–703.
[56] Ucero AC, Benito-Martin A, Fuentes-Calvo I, Santamaria B, Blanco J, Lopez-Novoa JM, et al. TNF-related weak inducer of apoptosis (TWEAK) promotes kidney fibrosis and Ras-dependent proliferation of cultured renal fibroblast. Biochimica et Biophysica Acta (BBA) - Molecular Basis of Disease 2013;1832(10):1744–55.
[57] Aukrust P, Halvorsen B, Yndestad A, Ueland T, Øie E, Otterdal K, et al. Chemokines and Cardiovascular Risk. ATVB 2008;28(11):1909–19.
[58] Herder C, Peeters W, Illig T, Baumert J, de Kleijn DPV, Moll FL, et al. RANTES/CCL5 and Risk for coronary events: results from the MONICA/KORA augsburg case-cohort, athero-express and CARDIoGRAM studies. PLoS One 2011;6(12):e25734.
[59] Al-Aly Z. Arterial calcification: a tumor necrosis factor-alpha mediated vascular Wnt-opathy. Transl Res. 2008 May;151(5):233-9. PubMed PMID: 18433704. Epub 2008/01/22.eng.